

Experimental study of the impact of ion orbit losses on the edge radial electric field at the ASDEX Upgrade tokamak

P. Cano-Megias^{1,2}, E. Viezzer^{2,3}, R. W. Brzozowski⁴, U. Plank⁴, M. Cavedon⁴, T. Happel⁴,
K. Höfler^{4,5}, D.J. Cruz-Zabala^{2,3}, R. Dux⁴, M. Griener⁴, J. Hobirk⁴, A. Jansen van Vuuren^{2,3},
T. Pütterich⁴, R. Chacartegui¹ and the ASDEX Upgrade Team

¹ Dept. of Energy Engineering, University of Seville, Seville, Spain

² CNA (U. Sevilla, CSIC, J. de Andalucía), Seville, Spain

³ Dept. of Atomic, Molecular and Nuclear Physics, University of Seville, Seville, Spain

⁴ Max-Planck-Institut für Plasmaphysik, Garching, Germany

⁵ Technische Universität München, Garching, Germany

Introduction. It is widely accepted that the formation of a strong shear in the edge radial electric field (E_r) aids the formation of an edge transport barrier and the transition into high confinement regimes [1]. However, the mechanism responsible for the generation of E_r has not been unambiguously identified yet. The ion orbit loss (IOL) mechanism is, amongst others, one of the possible candidates for E_r generation close to the plasma boundary, due to the non-ambipolar loss of ions executing orbits across the separatrix [2-4]. In this work we present the results of dedicated experiments that have been carried out to study the impact of IOL on E_r at the ASDEX Upgrade tokamak. The experimental results are compared to analytic calculations using a geometrical model [5,6], which allows us to determine the relative strength of IOL.

Control variables. In these experiments, the ion ∇B drift direction and the X-point triangularity (δ_x) are considered as the main actuators for the design of scenarios that maximize and minimize IOL, as discussed below:

∇B drift direction in relation to the X-point: This is the main actuator to affect IOL. Thermal IOL are expected to be higher in favourable configurations (∇B drift towards the active X-point) due to the asymmetry in the parallel connection length ($L_{||}$) with the ∇B drift direction [5-7]. In the unfavourable ∇B drift configuration, $L_{||}$ is longer than in favorable configuration. Given the same plasma conditions (same collisionality), particles will have a higher probability to undergo collisions and scatter out of the loss cone before completing a loss orbit in the unfavourable configuration. This results in a higher effective collisionality and lower IOL in unfavourable configuration in comparison to the favourable configuration.

X-point triangularity (δ_x) [6,8,9] – The closeness of the X-point to the low field side (LFS) influences orbital access to the X-point. When the X-point is closer to the LFS (low δ_x), the

probability of loss is higher, as particles will need a lower energy to intersect the X-point and get lost compared to a higher δ_X equilibrium. This is expected to be a 2nd order effect for IOL compared to the ∇B drift direction in relation to the X-point.

Experiment overview. Matching L-mode experiments in forward and reversed field, both in Upper (USN) and Lower (LSN) Single Null ($|I_p| = 0.6$ MA, $|B_t| = 2.5$ T) have been carried out at the AUG tokamak for a complete comparison. The scenarios have been designed to maximize (favourable configuration, low δ_X) and minimize (unfavourable configuration, high δ_X) ion orbit losses. In the middle of the flat-top of the discharges, a scan is performed in δ_X . Note that a 2nd scan was added in #38552 (resulting in 3 triangularity phases). The core density was feedback-controlled at $4.5 \cdot 10^{19} \text{ m}^{-3}$. The magnetic field, plasma current, input power (P_{ECRH} [MW]), δ_X and type of configuration are summarized in table 1.

Discharge	#37360		#37362		#37416		#38552		
IOL case	~	Max	Min	~	Min	~	~	Max	Max
δ_X	0.440	0.200	0.479	/	0.462	0.233	0.474	0.213	0.122
Conf., ion ∇B drift	USN, Up		LSN, Up		USN, Down		LSN, Down		
$I_p / B_t / P_{\text{ECRH}}$	-0.6 / 2.5 / 0.7		-0.6 / 2.5 / 1.4		0.6 / -2.5 / 1.4		0.6 / -2.5 / 0.4		

Table 1. Plasma parameters of the discharges designed and analysed in this work relevant for the study of ion orbit losses. The cases labelled as ‘~’ represent intermediate cases. The low δ_X phase in discharge #37362 was unstable and is excluded from the analysis.

Experimental measurements of E_r . The E_r profile was measured using active He II spectroscopy (HES) [10] and Doppler reflectometry (DR). The profiles for all cases are shown in Fig. 1. The offset between the DR and HES data is believed to be a diagnostic effect, due to a loss of alignment of the HES optical head during the experimental campaign. A correction for this effect is currently being assessed. Note that the overall trends are consistent for both diagnostics. The E_r profiles are compared to the ion pressure gradient term ($\nabla p/n$, being p the ion pressure gradient and n the electron density, assuming $n_i \sim n_e$) to quantify the impact of the change in the kinetic profiles on E_r , also shown in Fig. 1. Note that

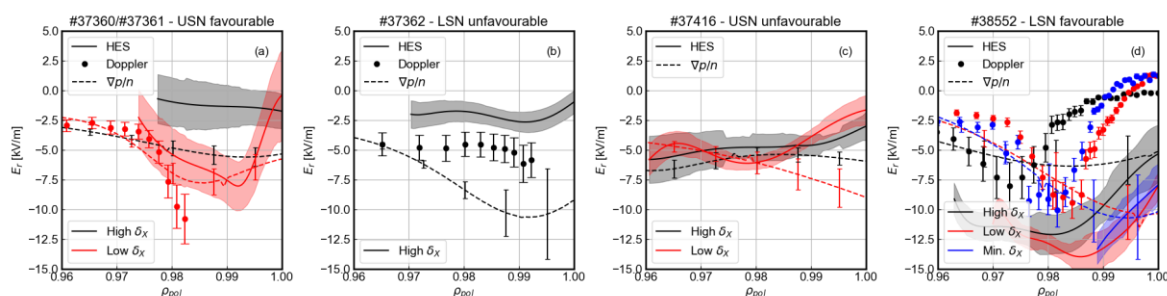


Figure 1. Radial electric field (E_r) profiles as measured by He II Spectroscopy (solid), Doppler reflectometry (circles) and ion $\nabla p/n$ (dashed). The colors indicate the X-point triangularity.

the changes in the $\nabla p/n$ during the δ_X scans are within error bars. The largest deviation of E_r from $\nabla p/n$ is observed in the minimum IOL case in reversed field (Fig. 1-b). This discrepancy is not expected to be an IOL effect and is currently being investigated.

Impact of X-point triangularity: there is a clear impact of δ_X in favourable cases (#37360 Fig. 1-a, #38552 Fig. 1-d). The E_r is deeper in the cases where we expect more IOL, namely, at the low δ_X . On the contrary, in the unfavourable case, the change of δ_X has no impact within experimental uncertainty (Fig. 1-c).

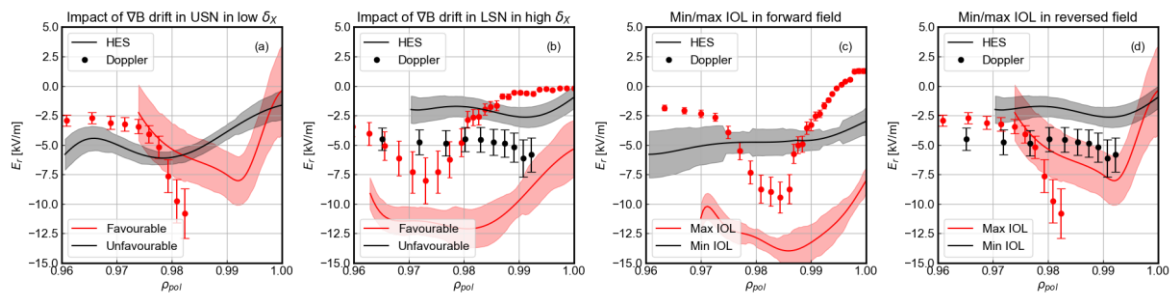


Figure 2. Comparison of the impact of the ∇B drift on E_r in (a) USN and low δ_X and (b) LSN and high δ_X . Comparison of E_r in the minimum (high δ_X , unfavourable) and maximum (low δ_X , favourable) ion orbit loss scenarios in (c) forward and (d) reversed field configurations.

Impact of the ∇B drift direction: the E_r shear is stronger in the favourable cases in LSN for all δ_X (see as example the high δ_X case in Fig 2-b) and in USN in the low δ_X (Fig. 2-a) compared to the unfavourable cases, in agreement with the expectation from IOL theory. In USN the ∇B drift does not have an impact on the E_r well within error bars for the high δ_X case (comparing black curves in Fig. 1-a and 1-c).

Comparison of minimum/maximum IOL cases: these comparisons are shown in Fig. 2-c and 2-d in forward and reversed field configurations, respectively. Clearly, in both field configurations the E_r well is deeper and features a stronger shear in the maximum IOL cases (low δ_X and favourable configuration). This implies that when the effects of both shorter path length and larger orbital access to the X-point combine, which lead to higher IOL, differences of more than 5 kV/m are observed in both field directions (Fig. 2-c and 2-d).

Ion orbit loss fractions. The experimental observations are compared to the analytic calculation of the loss fraction (F_{loss}) as $F_{Loss} = 1/\sqrt{\pi} \int_{-1}^1 (\Gamma(3/2, \epsilon_T) - \Gamma(3/2, \epsilon_U) + \Gamma(3/2, \epsilon_L)) d\zeta$, where Γ is the upper incomplete gamma function, ζ the pitch angle, ϵ the energy normalized by the ion temperature and T, L and U refer to the unbounded and bounded loss cone regions [5]. In these calculations, the loss cone is assumed to be empty and the

collisional processes (i.e. the increased effective collisionality in unfavourable configuration) are not included. Therefore, the calculations provide an upper limit for the strength of IOL and do not yet address a comparison of favourable versus unfavourable cases. The experimental kinetic

profiles, E_r profiles and magnetic geometries are used for the calculation. Fig. 3-a and 3-b show the impact of δ_X on F_{loss} in the favourable scenarios. When the E_r well is small ($|E_r| \lesssim 10$ kV/m, as in #37360 and #37416), F_{loss} increases when δ_X decreases, consistent with the deeper E_r measured experimentally at low δ_X (Fig 3-b). For deeper E_r wells ($|E_r| \gtrsim 10$ kV/m, as in #38552), the E_r is deep enough to mitigate IOL. In this case, the steepening of E_r during the δ_X scan suppresses an increase in IOL, such that there is no significant change in F_{loss} with δ_X as shown in Fig 3-a.

Conclusions. The impact of δ_X and ∇B drift direction on the E_r has been quantified in L-mode scenarios that maximize and minimize IOL. When both actuators act together, there is a measurable variation in the E_r aligned with the expectation from IOL theory, while their individual impact on E_r is not conclusive. Regarding the impact of the ∇B , we observe that the E_r well steepens in favourable configurations in LSN at all δ_X and USN at low δ_X compared to unfavourable configurations. However, the ∇B drift has no clear effect on E_r in USN at high δ_X . Lower δ_X coincides with deeper E_r wells as expected from the IOL model in favourable cases. In the unfavourable case, δ_X does not play a role within the experimental uncertainty. Future work will focus on the inclusion of collisional processes in the calculation of F_{loss} , which will allow a comparison of the favourable and unfavourable cases.

Acknowledgements. This work received funding from the Spanish Ministry of Science, Innovation and Universities (grant FPU17/06273). This work has been carried out within the framework of the EUROfusion Consortium and has received funding from the Euratom research and training programme 2014-2018 and 2019-2020 under grant agreement No 633053. The views and opinions expressed herein do not necessarily reflect those of the European Commission.

References

- | | |
|--|--------------------------------------|
| [1] Biglari H. et al Phys. Fluids B 1990 | [6] R.W. Brzozowski, PhD thesis 2021 |
| [2] KC Shaing et al, PRL 1989 | [7] KC Shaing et al, PoP 2002 |
| [3] K Miyamoto, NF 1996 | [8] DJ Battaglia et al NF 2013 |
| [4] CS Chang et al PRL 2017 | [9] Y Nishimura et al, PoP 2020 |
| [5] R.W. Brzozowski et al, PoP 2019 | [10] U. Plank, PhD thesis 2021 |

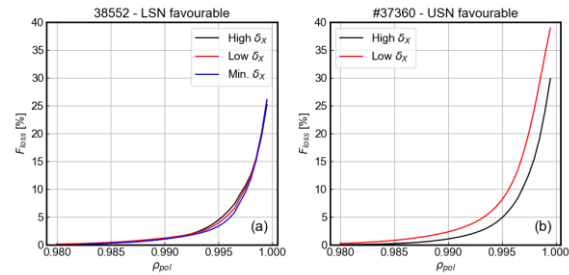


Figure 3. Loss fraction for the favourable cases in forward (a) and reversed field (b) for different δ_X .